Generation and characterization of radiolabelled nanosized carbonaceous aerosols for human inhalation studies

Jérémie Pourchez, Iolanda M.D. Albuquerque-Silva, Michèle Cottier, Anthony Clotagatide, Laurent Vecellio, Marc Durand, Francis Dubois

Generation and characterization of radiolabelled nanosized carbonaceous aerosols for human inhalation studies

Jérémie Pourchez[a,b,c], Iolanda M. D. Albuquerque-Silva[a,b,c], Michèle Cottier[a,c,d,e,f], Anthony Clotagatide[e], Laurent Vecellio[g,h], Marc Durand[a,c,i], Francis Dubois[a,c,d,e,f]

[a] LINA, EA 4623, F-42023, Saint-Etienne, France

[b] Ecole Nationale Supérieure des Mines de Saint-Etienne, Centre Ingénierie et Santé, F-42023, Saint-Etienne, France

[c] SFR IFRESIS, F-42023, Saint-Etienne, France

[d] Université Jean Monnet, Faculté de Médecine, F-42023, Saint-Etienne, France

[e] CHU de Saint-Etienne, F-42055, Saint-Priest en Jarez, France

[f] Université de Lyon, F-42023, Saint-Etienne, France

[g] DTF Aerodrug – Diffusion Technique Française, Tours, France

[h] INSERM U1100-EA6305, Université François Rabelais, Tours, France

[i] Centre Hospitalier Emile Roux, F-43012, Le Puy en Velay, France

Correspondence to: Jérémie POURCHEZ, Ecole Nationale Supérieure des Mines de Saint-Etienne, Centre Ingénierie et Santé, 158 Cours Fauriel 42230, France. Telephone / Fax number: + 33 4 77 42 01 80 / +33 4 77 49 96 94, mail: pourchez@emse.fr

ABSTRACT

New insights on the output of a commercial Technegas generator were proposed in order to optimize the generation of a radioactive nanosized aerosol for human inhalation studies. Parameters influencing Technegas generated aerosols (*i.e.* gaseous atmosphere, generation temperature and storage duration) were analyzed by a combination of size-fractionation and gamma-scintigraphy detection to determine the aerosol aerodynamic-related distributions. It was found that the total radioactivity per mass and number concentrations of aerosols was mostly influenced by the burn temperature, while the radiolabelling of particles was mostly driven by their surface area. ^{99m}Tc labeled nanosized carbonaceous primary particles appear mainly to result from nucleation/condensation of the supersaturated vapor during the burning step, and then coalesce into larger particles due to coagulation processes during the residence time in the expansion chamber. We showed that the burn temperature and the aerosol residence time were the main parameters influencing the particle size distribution. Under optimized operating conditions, the amount of radiolabelled nanoparticles substantially increased since the radioactivity median aerodynamic diameter was reduced by half (250 nm - GSD of 2.5) compared with the standard operating conditions of the Technegas generator (450 nm - GSD of 3.4).

KEYWORDS: Technegas; ELPI; radiolabelled nanosized aerosols

MAIN TEXT

1. Introduction

Radiolabelled aerosols are widely used to study airborne particle deposition patterns in the lung as well as lung clearance (Möller et al., 2006; Sanchez-Crespo et al., 2011; Carvalho et al., 2011). Among all the radiolabelled aerosols clinically used in patients, one of the most convenient is the “Technegas technique” widely used to perform lung ventilation scintigraphy as a diagnostic technique in nuclear medicine. The aerosol produced is commonly known as Technegas, an ultrafine suspension of carbon particles labeled with technetium (^{99m}Tc). Technegas preparation takes place in a specially designed machine, called the Technegas generator, where a solution of sodium pertechnetate is loaded into a graphite crucible and evaporated until dry. Technegas is then generated by heating to 2550 °C in an atmosphere of pure argon. The number size distribution of Technegas particles is mainly below 100 nm (Vita Medical Ltd., 2000). Since more than 2 decades, this radioactive aerosol is regularly used as a ventilation scintigraphy agent, and the device is approved for human application without any toxicological issues (Jögi et al., 2010, Senden et al., 1997; Lloyd et al., 1995; Burch et al., 1986). Due to the short half-life of ^{99m}Tc (6.02 h), the radiation dose can be kept low (< 0.1 mSv) even though the resulting high activities allow high quality gamma-camera imaging in nuclear medicine.

Under standard operating conditions, the Technegas generator produces airborne particles with leaching rates >10% which are too high for clearance studies. Since NaCl contained in the ^{99m}Tc-eluate also evaporates and condenses during the burning step, the particles have hygroscopic properties and the radiolabel leaches from them. Recently Moeller et al. (2006) proposed several modifications to the operating conditions of the Technegas generator to avoid these drawbacks such as

48 the use of NaCl free ^{99m}Tc-eluate. In addition the particles could be labeled by ^{111}In
49 (Sanchez-Crespo et al., 2011) or $^{68}GaCl_3$ (Borges et al., 2011) instead of ^{99m}Tc to
50 extend the investigation time of clearance studies from 1 day to a few weeks.

51 Although it is generally accepted that the Technegas generator produces a
52 smaller particle size than other conventional radiolabelled aerosols, few data are
53 available about its particle size characteristics. To the best of our knowledge no data
54 have yet been reported on the relationship between radioactivity aerodynamic
55 diameter (AMAD) although this parameter is crucial to assess deposition patterns.
56 Even the median diameter remains poorly defined in the range from about 200 to 400
57 nm (Borges et al. 2011, Lemb et al., 1993; Strong and Agnew, 1989; Möller et al.,
58 2006). In fact, clinical experiments in nuclear medicine indicate that radiolabelled
59 Technegas particles are likely to impact on obstructions within the respiratory tract,
60 which is a behavior typically attributed to micrometer sized aerosols (Jögi et al.,
61 2010).

62 The radiolabelling mechanism and radiolabelling efficiency of airborne particles
63 related to their aerodynamic size also remain poorly understood. Therefore, this
64 study aims at new insights on the output of a Technegas device generating ^{99m}Tc
65 labeled nanosized carbonaceous aerosols. The physical properties of the airborne
66 nanoparticles in term of radiolabelling efficiency, number, mass and surface area
67 concentrations are characterized by using a combination of size-fractionation and
68 gamma-scintigraphy detection. Based on the experimental methodology previously
69 developed by Moeller *et al.* (2006), we also propose a better understanding of the
70 effect of Technegas generator operating conditions on the characteristics of the
71 radiolabelled particle size distributions. Finally, we also describe optimal operating
72 conditions to generate radiolabelled carbonaceous nanoparticles.

2. Material and methods

The generation of Technegas was first reported in 1986, as a simple process consisting of evaporating Technetium (^{99m}Tc) containing eluate in a graphite crucible at 2500°C (Burch et al., 1986). The Technegas generator is essentially a miniature high temperature furnace (Figure 1). It uses a combination of graphite in an argon atmosphere to chemically reduce the pertechnetate ion TcO_4^- contained in the ^{99m}Tc sodium pertechnetate solution to metallic technetium (Tc), and then produce metallic aerosol particles by vaporizing both carbon and technetium elements. The inert atmosphere is critical to produce pure carbon or metallic aerosols (Evans et al., 2003). The crucible is the source of graphite vapour which ultimately coats the technetium metal. An AC electrical current passes through two conducting substrates (electrodes and crucible) possessing relatively low vapour pressure. The metallic aerosol forms first by nucleation/condensation of the vapour, followed by agglomeration of airborne nanoparticles composed of hexagonal platelets of metallic technetium (^{99m}Tc) closely encapsulated with a thin layer of graphitic carbon. During Technegas production, particles are not equally radiolabelled. The rapid volatilization of the species involved and the surface passivation of the resulting metallic aerosol are major factors influencing particles formation and stabilization, which may proceed differently according to particle size distribution (Senden et al., 1997).

In this work, the Technegas generator (Cyclomedica Pty Ltd, Australia) was operated in its “maintenance mode”, which allows modifying its operating conditions. A pyrometer was coupled to the generator in order to control burn temperature. For aerosol production, a standard graphite crucible was previously humidified with 99% ethanol in order to increase its wetability and then filled with a 200MBq ^{99m}Tc-sodium pertechnetate solution placed in the Technegas generator chamber. The produced

aerosol was subsequently analyzed by an electrical low pressure impactor (ELPI, Dekati Ltd., Finland) and a gamma camera (Millenium, GE, USA), to determine the particle size distribution both by weight, number, surface area and radioactivity. The NaCl content in ^{99m}Tc-eluate was also evaluated with respect to its influence on the final particle size distribution. All experiments were performed in triplicate and statistically analyzed (unpaired t-test).

2.1 Aerosol generation parameters

Under standard clinical operating conditions, the aerosol production is initiated through the "*simmer"* stage, which is characterized by a modification of the generator chamber atmosphere by argon flushing and a slight heating of the crucible up to 80°C for a 6 minute duration (Vita Medical Ltd., 2000). Under these conditions, the ^{99m}Tc eluate is evaporated to dryness, providing an intimate contact between the crucible and the species of ^{99m}Tc-sodium pertechnetate solution (Senden et al., 1997). Subsequently, the *"burn"* stage begins in which the crucible is finally heated to 2550°C for 10 seconds (Vita Medical Ltd., 2000). This heating leads to technetium and carbon evaporation with subsequent condensation and aerosol formation. It is therefore reasonable to conclude that the major parameters influencing aerosol generation are the burn temperature, the duration of the simmer and the burn stages. Another important parameter is the residence time in the expansion chamber. During clinical procedures, a delay (*i.e.* a residence time in the expansion chamber) occurs between Technegas generation and its delivery to the patient. This delay is usually on the order of 2 minutes. During the residence time in the expansion chamber, particles are able to coagulate and agglomerate, with a significant impact on the

subsequent size distribution of the radioactive aerosol delivery to the patient (Möller et al., 2006).

The standard clinical parameters for Technegas production are prescribed as 6 minutes of simmering, followed by 10 s of burning at 2500°C followed by 2 minutes of residence time. However, in order to reduce the consumption of the generator electrodes, in this work the standard burn stage duration was reduced to 5 seconds instead of 10. The proposed change of operating conditions of the Technegas generator was based on a previous study from Möller et al. (2006). The analyses of particle size distribution were performed by varying each generation parameter: (I) simmer duration (6 – 15 min); (II) burn temperature (1900 – 2800°C); (III) burn duration (2 – 15s) and (IV) aerosol residence time (0.5 – 10 min). The operating conditions of the Technegas generator were summarized in Figure 2.

2.2 Particle size distributions

Aerosol size distributions were determined using the ELPI low pressure impactor. The ELPI classifies by aerodynamic diameter, in 12 size fractions ranging from 10 µm to 7 nm (Virtanen et al., 2001; Marjamäki et al., 2000). The number concentration was converted to mass and surface area concentrations assuming the graphite crucible density (2.13 $g.cm^{-3}$) for the particles. Differential distributions and normalized cumulative distributions are shown in accordance with the European standard EN 13544-1 for respiratory therapy equipment, which is widely employed for pharmaceutical aerosols. The cumulative distributions were normalized, *i.e.* data were expressed in % where 100% corresponds to total radioactivity (from gamma-camera measurements) or total mass/number/surface area (from ELPI calculations) deposited on all the 12 collection plates of the cascade impactor.

147 *2.3 Radioactivity measurements*

148 A combination of ELPI size fractionation and gamma scintigraphy detection
149 was used to determine the aerodynamic radioactivity size distribution. For this
150 purpose, the aerosol was collected on cellulose substrates inserted on the collection
151 plates of the impactor. The radioactivity of airborne particles deposited on each
152 collection substrate was determined by gamma scintigraphy imaging during a 2
153 minutes acquisition time. The distribution of radioactivity is presented versus the ELPI
154 stage mid-point aerodynamic diameter.

155

156 *2.4 Electron microscopy observations and chemical analysis*

157 Field Emission Gun Scanning Electron Microscopy (FEG SEM, Jeol JSM
158 6500F) was used to analyze the Technegas particles deposited within the ELPI
159 stages. SEM observations coupled with image analysis also provided a mean
160 geometric particle diameter for each size class of the ELPI.

161 The sodium and chloride concentrations in the Tc-eluate were obtained by ion
162 chromatography with a Dionex apparatus composed of a GP50 pump, a CS12A
163 column for cation analysis, a AS11HC column for anions, a CD conductometric
164 detector and a UV-visible detector. The presence of NaCl in the airborne particles
165 was characterized using energy-dispersive X-ray spectroscopy (EDX) coupled with a
166 scanning electron microscope. The EDX analytical technique was used for the
167 elemental analysis of airborne particles (except carbon and technetium elemental
168 detection). The sodium, chloride and technetium content of airborne particles were
169 measured using X-ray photoelectron spectroscopy (XPS). XPS is a quantitative
170 spectroscopic technique for the elemental composition.

171

3. Results

3.1 Technegas aerosol under standard operating conditions

A linear correlation was found between the geometric diameter of particles calculated by image analysis from SEM images and the corresponding mid-point aerodynamic diameter of the ELPI stage (Figure 3). Results show a particle distribution composed of a predominantly carbonaceous nature for the ultrafines particles (in the 30-300 nm size range) and the dominant NaCl content of the micron sized particles (Figure 3). The sodium chloride content of numerous micrometer sized particles was clearly put in evidence by EDX spectroscopy during SEM observations and XPS analysis. On the ELPI stages corresponding to mid-point aerodynamic diameters higher than1 µm, SEM images also show the presence of coagulated carbonaceous particles (data not shown but similar to Figure 7), which precluded the correct determination of their geometric diameter, leading to slight deviations from ELPI measurements even if the overall correlation remains quite good.

The particle size distributions of the aerosol obtained under standard operating conditions used in clinical routine are first presented in terms of number, surface area, mass and radioactivity (Figure 4). Number distributions are dominated by nanoparticles with aerodynamic diameters lower than 100 nm with a Count Median Aerodynamic Diameter (CMAD) of 40 nm (GSD of 2.9). However, radioactivity distributions indicate that radiolabelled particles are mostly distributed in the range between 100 nm and 1 µm, providing an Activity Median Aerodynamic Diameter (AMAD) of 450 nm (GSD of 3.4). Radioactivity distributions were found to be in good accordance with surface area distributions, characterized by a Surface Median Aerodynamic Diameter (SMAD) of 540 nm (GSD of 2.1). Finally, mass distributions

showed particles exclusively distributed in the size range above 100 nm, leading to a Mass Median Aerodynamic Diameter (MMAD) of 820 nm (GSD of 2.7) .

The combination of aerodynamic and radioactivity measurements provides new insights into the radiolabelling process. A radiolabelling efficiency was defined as the ratio between activity (in fact radioactivity, in Bq) and mass from particles deposited on each ELPI stage. According to Figure 5, particle radiolabelling is most efficient in the nanometer range and than decreases continuously with aerodynamic diameter.

The electric charge level of the freshly generated airborne Technegas particles was also checked by ELPI (using the ELPI with the corona charger OFF) in order to verify that the original electric charge of the particles does not affect the ELPI detection based on current measurement. Results show that the aerosol particles are weakly charged and that the charge distribution depends to the aerodynamic particle size. Particles are positively charged (13 fC) for sizes from 28 to 262 nm, negatively charged (-12 fC) in the range 262 nm to 1.6 µm, and finally neutral for sizes greater than 1.6 µm. In this case, the corona charger produces a sufficient amount of positive ions to first neutralize and then charge the particles normally up to 7500 fC, 500 times higher than the original electric charge of the particles. Furthermore, the use of cellulose substrates for particles recovery on the ELPI stages has no significant influence ($p < 0.05$) on the Technegas particle size distribution. Both methods generate aerosol with an AMAD of 445 (GSD of 3.0) and 450 nm (GSD of 2.7) respectively (Table 1).

3.2 Technegas aerosol characteristics under modified operating conditions

We now show that the modified operating conditions significantly influence the particle size distribution (Figure 6). Results are also summarized as mean of AMAD

and GSD in Table 2. An increased simmer increases the amount of nanoparticles significantly. 15 minutes of simmering (instead of 6 min under standard clinical operating conditions) increase the nanoparticle population by 10%, leading to a reduction of the Technegas AMAD from 450 to 305 nm. Increasing the burn duration from 2 to 10 seconds also reduces the AMAD from 500 to 370 nm. However, increasing the burn duration beyond 10 seconds does not have a significant influence on the aerosol AMAD.

The burn temperature of the crucible, and the aerosol residence time in the expansion chamber, appear to be the main parameters affecting aerosol generation. Therefore, either an increase of burn temperature or a decrease of residence time leads to a substantial reduction of aerosol AMAD and an increased amount of radiolabelled nanoparticles. Increasing the burn temperature from 1900°C to 2800°C leads to a decrease of AMAD from 510 to 270 nm. A decrease of residence time from 10 minutes to 0.5 minutes gave a decrease of AMAD from 540 to 285 nm. SEM observations showed that the morphology of aerosols particles was also highly dependent on their residence time. Therefore, particle coagulation and agglomeration were visibly reduced for small aerosol residence times (30 seconds) but manifestly present for long residence times (10 minutes) (Figure 7).

Moreover, the total amount of aerosol radioactivity, *i.e.* the number of technetium atoms fixed on carbonaceous particles, was also strongly influenced by the generation parameters, especially by the burn temperature (Figure 8). Thus, a reduction of temperature to 1900°C causes a significant reduction in total radioactivity, up to 4 times lower than in standard clinical operating conditions.

Finally, the radiolabelled particle size was mostly affected by the burn temperature. Thus, an optimization of the generation method is proposed based on

246 adjustments of the burn temperature, in order to maximize the production of
247 radiolabelled nanoparticles. This optimized method of radiolabelled aerosol
248 production was performed by two consecutives burn stages, using both extremes of
249 burn temperature of the generator: 5 second burn at 1900°C followed by 5 second
250 burn at 2800°C. The optimized radiolabelled aerosol showed an aerodynamic particle
251 size distribution with an AMAD of 250 nm (GSD of 2.5), about 2 times smaller than
252 standard Technegas, but to a 15% increase of the radiolabelled nanoparticles (Figure
253 9).

254 Once the optimized conditions for Technegas production were determined, the
255 influence of the NaCl content on Tc-eluate was analyzed. Ionic chromatography
256 confirms the very low NaCl concentration (in the range 20-100 mg/L) of the NaCl free
257 Tc-eluate, by comparison with the NaCl concentration of 9 g/L for NaCl Tc eluate.
258 Results further prove that an initially NaCl-free eluate did not significantly modify the
259 particle size distribution (AMAD of 200 nm) (Figure 9).

260

4. Discussion

In the present study, based on a methodology combining radioactivity measurements and aerodynamic size fractionation, for the first time the Technegas size distributions are expressed in terms of size-related radioactivity, characterized by AMAD. Using ELPI based calculations, the aerosol was also characterized by its CMAD, SMAD and MMAD. These calculations are based on positive ion active surface areas measured by ELPI, and the masses of spheres with diameter equal to the midpoint aerodynamic values (D_a) of each stage. Active surface area is generally defined as the surface of a particle that is involved in interactions with the surrounding gas (Fuchs, 1963). Thus, the ELPI provides a real time size-selective (aerodynamic diameter) active surface-area concentration. In this sense the surface area measured by the ELPI is an active surface area quite relevant to describe Tc-carbone interactions. The active surface area distribution appears to be the most appropriate form to describe the radiolabelled particles distributions since a good correlation is observed between surface area and radioactivity cumulative distributions (Figure 4). This original data demonstrates that particle radiolabelling is mostly proportional to their active surface area, rather than particle number or mass. In other words, the quantity of technetium atoms fixed on the carbonaceous particles is mainly dependent to their active surface area.

Further, the Technegas MMAD (820, GSD of 2.7) was found to be almost 20 times higher than its CMAD, which trivially indicates that Technegas nanoparticles, although abundant in number, are not significant in mass. However, activity measurements provide an AMAD (450 nm, GSD of 3.4) corresponding to the half of Technegas MMAD, which can be explained by the fact that its nanoparticles, although insignificant in mass, have a considerable radioactivity. The radiolabelling

efficiency of Technegas particles, expressed by means of activity-to-mass ratio, also indicates that particle radiolabelling was more efficient on the nanometric scale (Figure 5). This result highlights the role played by particle surface area during radiolabelling. In this sense, the higher active surface area to volume ratio of nanoparticles (compared to micrometric particles) can easily explain the continuous decrease of radioactivity to mass ratio with the increase of aerodynamic diameter. The remarkable radiolabelling efficiency of nanoparticles can also be explained by their mode of production. In previous work, Senden et al. (1997) observed that the radioactivity only leaves the crucible at the melting point for technetium (2250 ± 50°C), which probably indicates that there is a passive mechanism of particle ejection from the crucible (i.e. the evaporation of the metal). Once in the vapor phase, technetium may condense as a metallic aerosol, being instantly passivated by condensed carbon (Senden et al., 1997).

Our data support the assumption that the generation of Technegas nanoparticles is driven by a mechanism quite similar to aerosol produced by spark discharge generators. Technegas nanoparticle generation could be therefore explained by a simultaneous ablation of technetium and graphite, caused by the striking of an alternative current arc from the thermionic plasma inside the crucible (Vita Medical Ltd., 2000). ^{99m}Tc labeled nanosized carbonaceous particles appear mainly to result from nucleation/condensation during the burning step followed by coagulation processes during the residence time in the expansion chamber. Nevertleless, these mechanisms are still not entirely proven and require further investigations.

All the operating conditions of the Technegas generator (*i.e.* simmer, burn duration, burn temperature and aerosol residence time) show an influence on the particle size distribution (Figure 6). A decrease of aerosols AMAD was observed with increasing

simmer and burn durations. These parameters apparently facilitate ablation and condensation phenomena and thus contribute to the AMAD reduction. Although the simmer and burn duration had some impact on the particle size distribution, stronger modifications were observed by adjusting on the residence duration in the expansion chamber and the burn temperature. Longer residence times obviously lead to coagulation and a higher AMAD (Table 2, Figure 7). This result confirms the relative instability of freshly radiolabelled nanoparticles over the timeshown in previous studies (Llyod et al.,1995, Möller et al., 2006). A noticeable reduction of AMAD from 510 nm (GSD of 3.0) to 270 nm (GSD of 2.7) was observed for an increase of burn temperature from1900°C to 2800°C. Furthermore, burn temperature was the parameter which had the strongest influence on the total aerosol radioactivity (Figure 8). As the burn temperature plays a major role on the output of Technegas device, an optimized method has been proposed which is based on a temperature of 1900°C followed by 2800°C to reduce the AMAD (Figure 9).

Finally, we demonstrate that the absence of sodium chloride in the initial pertechnetate eluate does not significantly modify the particle size distribution (AMAD of 200 nm) compared to usual NaCl pertechnetate eluate (Figure 9). This result suggests that NaCl crystals generated using NaCl Tc-eluate are poorly radiolabelled compared to carbonaceous nanoparticles. Previous studies (Moller et al., 2006, Wiebert et al., 2006a, 2006b) demonstrated that the removal of NaCl from ^{99m}Tc-sodium pertechnetate also yielded low leaching rates of radiolabel from particles of below 4% within 24h, and also guaranteed non-hygroscopic aerosol properties. The removal of NaCl from the Tc-eluate therefore seems to have several advantages.

Conclusion

The particle size distribution of the Technegas generator has been characterized from combined measurements of radioactivity (using a gamma camera) and aerodynamic sizing (using ELPI). Under standard clinical operating conditions, Technegas shows a radioactivity median aerodynamic diameter (AMAD) of 450 nm (GSD of 3.4). The particle size distribution and the total radioactivity of the aerosol are mostly influenced by the burn temperature. We proposed an optimized procedure to produce radiolabelled nanoparticles using the commercial Technegas generator consisting of two consecutive burns at 1900°C and 2800°C. Under optimized conditions, the median diameter of Technegas can thereby be reduced by half (250 nm), together with a substantial increase of its radiolabelled nanoparticle population.

Aerosols containing a greater amount of radiolabelled nanoparticles may permit better particle deposition within the respiratory tract. In this context an improvement of lung ventilation scintigraphy in nuclear medicine is conceivable. These new insights appear also valuable to assess deposition patterns of well-defined nanoparticles within the respiratory tract, in the case of inhalation toxicology and drug delivery by aerosol therapies. Finally, the proposed approach to optimize the generation of radioactive nanosized aerosol using the technegas generator can be coupled with other previous modifications such as a higher stable radiolabelling over time by removing NaCl from the Tc-eluate, or the possibility of $^{111}In/^{68}GaCl_3$ labbelling, to enhance alveolar pattern deposition and provide potential clinical improvements on inhalation studies.

ACKNOWLEDGEMENTS

The authors would like to acknowledge the financial support of the Regional French Association for Aid to Chronic Respiratory Failure Patients (ARAIR), Saint-Etienne Métropole and the Conseil Général de la Loire, as well as the helpful conversations and experimental support of the Cyclopharma Laboratoires (France). The authors would like also to thank the editor for all corrections and helpful comments which greatly contribute to this paper. Finally, special thanks to Laurent Navarro (Ecole Nationale Supérieure des Mines de Saint-Etienne, Centre Ingénierie et Santé, France) for his contribution to the image analysis and algorithm development on SEM images.

REFERENCES

Borges, J.B., Velikyan, I., Langström, B., Sörensen, J., Ulin, J., Maripuu, E., Sandström, M., Widström, C., Hedenstierna, G. (2011). Ventilation distribution studies comparing Technegas and "Gallgas" using $^{68}GaCl_3$ as the label. *Journal of Nuclear Medicine*, 52, 206-209.

Burch, W.M., Sullivan, P.J., McLaren, C. (1986). Technegas – a new ventilation agent for lung scanning. *Nuclear Medicine Communications,* 7, 865-871.

Carvalho, T.C., Peters, J.I., and Williams, R.O. (2011) Influence of particle size on regional lung deposition – What evidence is there? *International Journal of Pharmaceutics*, 406, 1-10.

Dekati Ltd. ELPI in pharmaceutical measurements. In: Dekati Ltd Application Note. 2007.

Evans, D.E., Harrison, R.M., Ayres J.G. (2003). The generation and characterization of elemental carbon aerosols for human challenge studies. *Journal of Aerosol Science*, 34, 1023-1041.

Fuchs, N. (1963) On the stationary charge distribution on aerosol particles in a bipolar ionic atmosphere. *Geofisica Pura e Applicata*, 56, 185-193.

392 Jögi, J., Jonson, B., Ekberg, M., Bajac, M. (2010). Ventilation-Perfusion SPECT with
393 99mTc-DTPA versus Technegas: A head-to-head study in obstructive and
394 nonobstructive disease. *Journal of Nuclear* Medicine, 51, 735-741
395
396 Lemb, M., Oei, T.H., Eifert, H., Günther, B. (1993). Technegas: a study of particle
397 structure, size and distribution. *European Journal of Nuclear Medicine*, 20, 576-579.
398
399 Lloyd, J.J., Shields, R.A., Taylor, C.J., Lawson, R.S., James, J.M., Testra, H.J.
400 (1995). Technegas and Pertechnegas particle size distribution. *European Journal of*
401 *Nuclear Medicine*, 22, 437-476
402
403 Marjamäki, M., Keskinen, J., Chen, D.R., Pui, D.Y.H. (2000). Performance evaluation
404 of the electrical low-pressure impactor (ELPI). *Journal of Aerosol Science*, 31, 249-
405 261.
406
407 Möller, W., Felten, K., Seitz, J., Sommerer, K., Takenaka, S., Wiebert, P., Philipson,
408 K., Svartengren, M., Kreyling, W.G. (2006). A generator for the production of
409 radiolabelled ultrafine carbonaceous particles for deposition and clearance studies in
410 the respiratory tract. *Journal of Aerosol Science*, 37, 631-644.
411
412 Sanchez-Crespo, A., Klepczynska-Nyström, A., Lundin, A., Larsson, B.M.
413 Svartengren, M. (2011). Indium-labeledultrafine carbon particles; a novel aerosol for
414 pulmonary deposition and retention studies. Inhalation Toxicology, 23,121-128.
415

Senden, T.J., Moock, K.H., Gerald, J.F., Burch, W.M., Browitt, R.J., Ling, C.D., and Heath, G.A. (1997). The physical chemical nature of Technegas. *Journal of Nuclear Medicine*, 38, 1327-1333.

Strong, J.C., Agnew, J.E. (1989). The particle size distribution of Technegas and its influence on regional lung deposition. *Nuclear Medicine* Communications, 10, 425-430.

Virtanen, A., Marjamäki, M., Ristimäki, J., Keskinen, J. (2001). Fine particle losses in electrical low-pressure impactor. *Journal of Aerosol Science,* 32, 389-401.

Vita Medical Ltd. Technegas Service Manual Document N°70305. 2000:P2-4.

Wiebert P., Sanchez-Crespo A., Falk R., Philipson K., Lundin A., Larsson S., et al. (2006a). No significant translocation of inhaled 35-nm carbon particles to the circulation in humans *Inhalation Toxicology* 18, 741–747.

Wiebert, P., Sanchez-Crespo, A., Seitz, J., Falk, R., Philipson, K., Kreyling, W. G., Moller, W., Sommerer, K., Larsson, S., and Svartengren, M. (2006b). Negligible clearance of ultrafine particles retained in healthy and affected human lungs. *European Respiratory Journal*, 28, 286-290.

TABLES LEGENDS

TABLE 1. Influence of generator mode and ELPI collection substrates on aerosols particle size distributions: radioactivity median aerodynamic diameters (AMAD) and geometric standard deviation (GSD).

TABLE 2. Radioactivity median aerodynamic diameters (AMAD) and geometric standard deviation (GSD) under standard clinical operating conditions, or under modified and optimized operating conditions (modified generation parameters in bold).

FIGURES LEGENDS

FIGURE 1. Schematic diagram of the Technegas generator.

FIGURE 2. Operating conditions of the Technegas generator: description of analyzed parameters.

FIGURE 3. EDX analysis coupled with SEM observation of ELPI stage showing carbonaceous nanoparticles (A) and NaCl crystals (B). Linear correlation between geometric diameter obtained by image analysis on SEM images and corresponding mid-point aerodynamic diameter determined by ELPI.

FIGURE 4. Aerodynamic size distributions of aerosol generated under standard clinical operating mode: differential distributions from ELPI calculations (top) and cumulative distributions from combined ELPI and gamma-camera measurements (bottom).**FIGURE 5.** Radiolabelling efficiency expressed as radioactivity per mass of particle.

FIGURE 5. Radiolabelling efficiency expressed as activity per particle mass.

FIGURE 6. Operating parameters influencing Technegas aerodynamic particle size distribution. Clinical operating conditions are used as a reference (distribution in black bold line).

FIGURE 7. SEM images of particles deposited on ELPI stage corresponding to mid-point aerodynamic diameter of 2.39 µm for residence times of (A) 30 seconds and (B) 10 minutes. Arrows indicate agglomerated particles.

FIGURE 8. Total radioactivity of evaluated radio-aerosols: influence of operating parameters (* : Values are not significantly different, $p<0.05$).

FIGURE 9. Technegas aerodynamic particle size distribution: comparison between standard clinical production, optimized production and optimized production using NaCl free-eluate.

FIGURE 1. Schematic diagram of the Technegas generator.

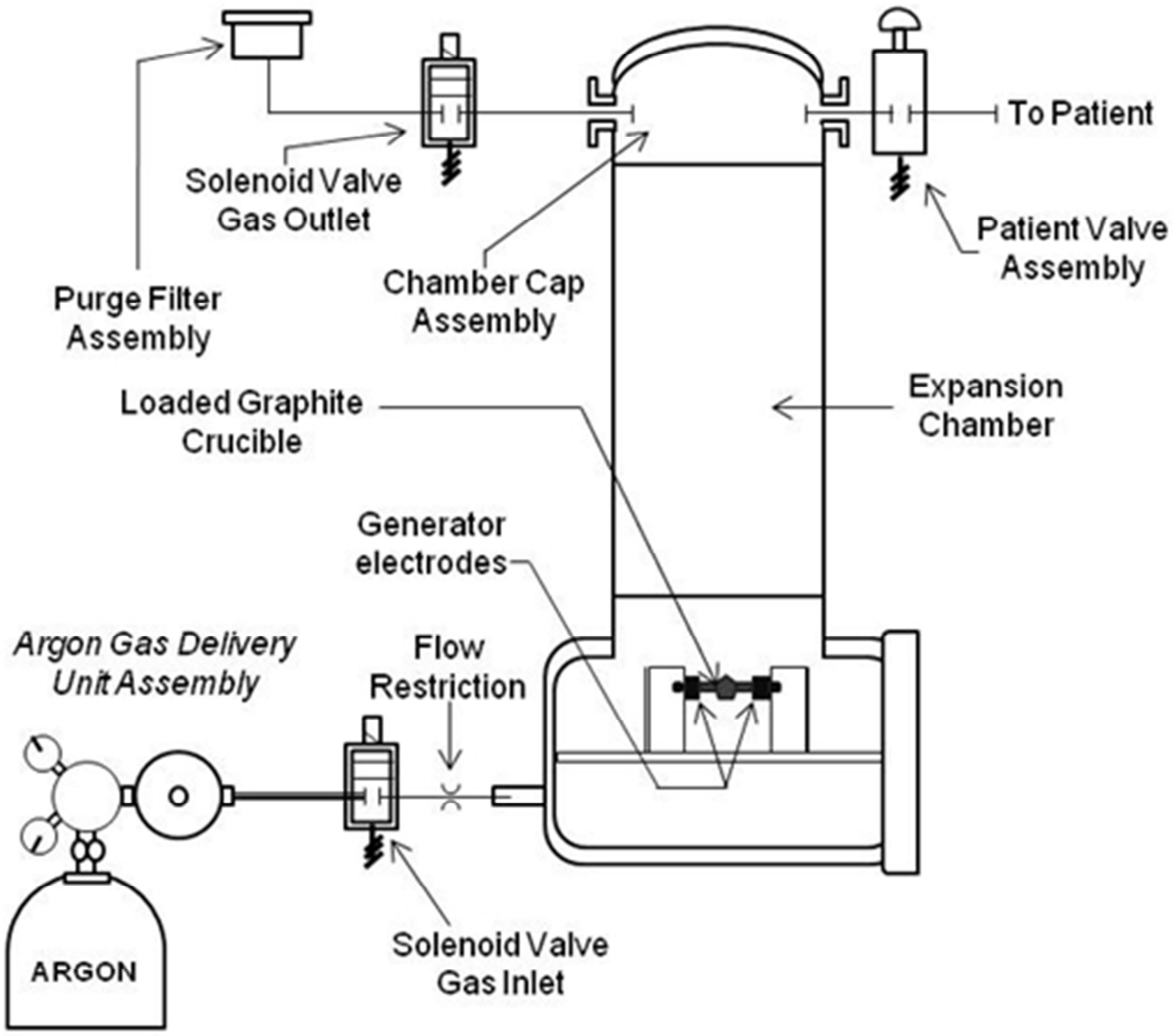

FIGURE 2. Operating conditions of the Technegas generator in the maintenance mode : description of analyzed parameters.

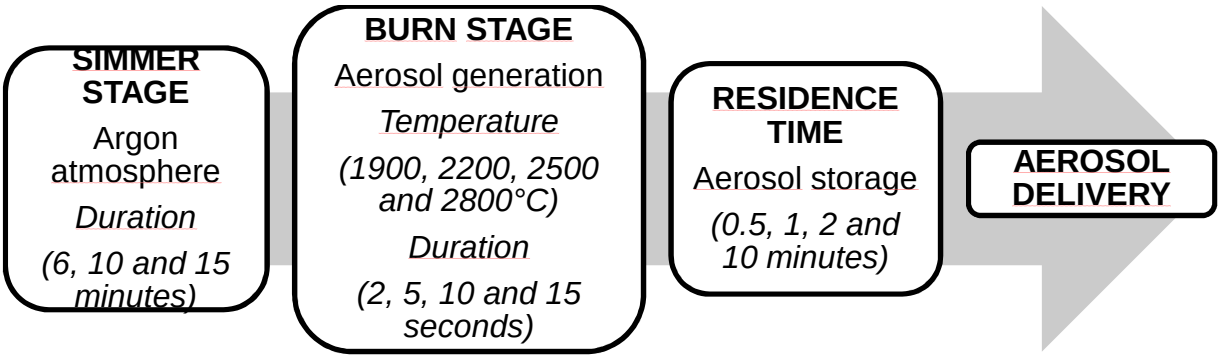

FIGURE 3. EDX analysis coupled with SEM observation of ELPI stage showing carbonaceous nanoparticles (A) and NaCl crystals (B). Linear correlation between geometric diameter obtained by image analysis on SEM images and corresponding mid-point aerodynamic diameter determined by ELPI.

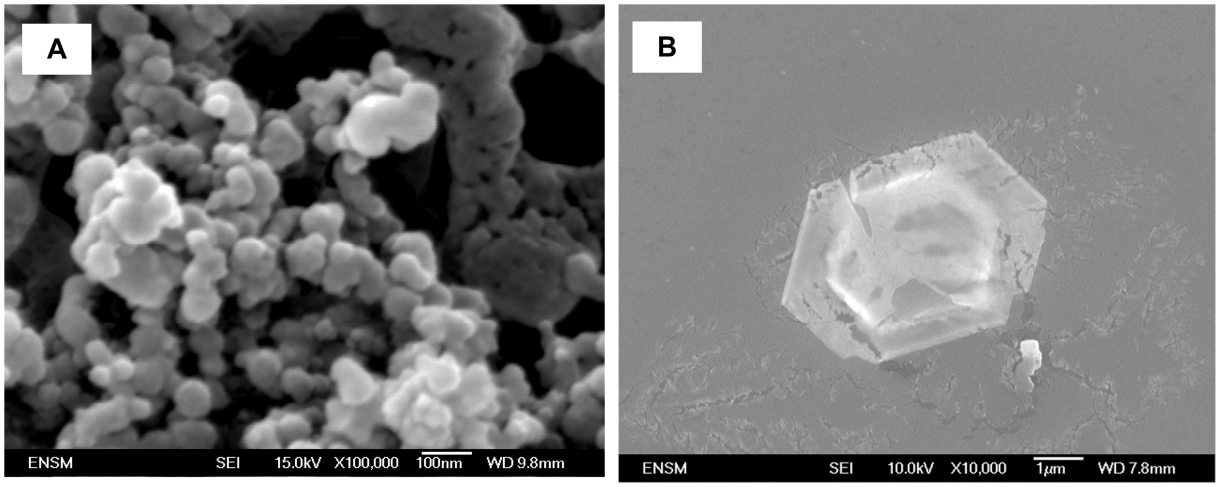

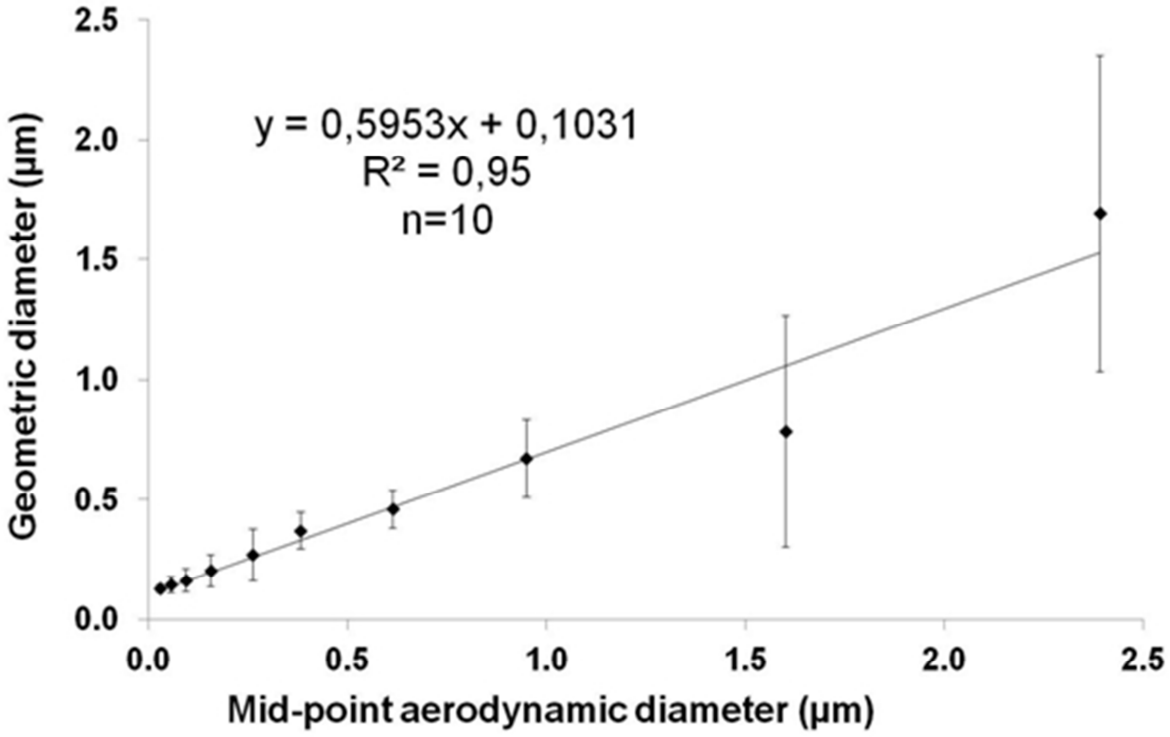

FIGURE 4. Aerodynamic size distributions of aerosol generated under standard clinical operating mode: differential distributions from ELPI calculations (top) and cumulative distributions from combined ELPI and gamma-camera measurements (bottom).

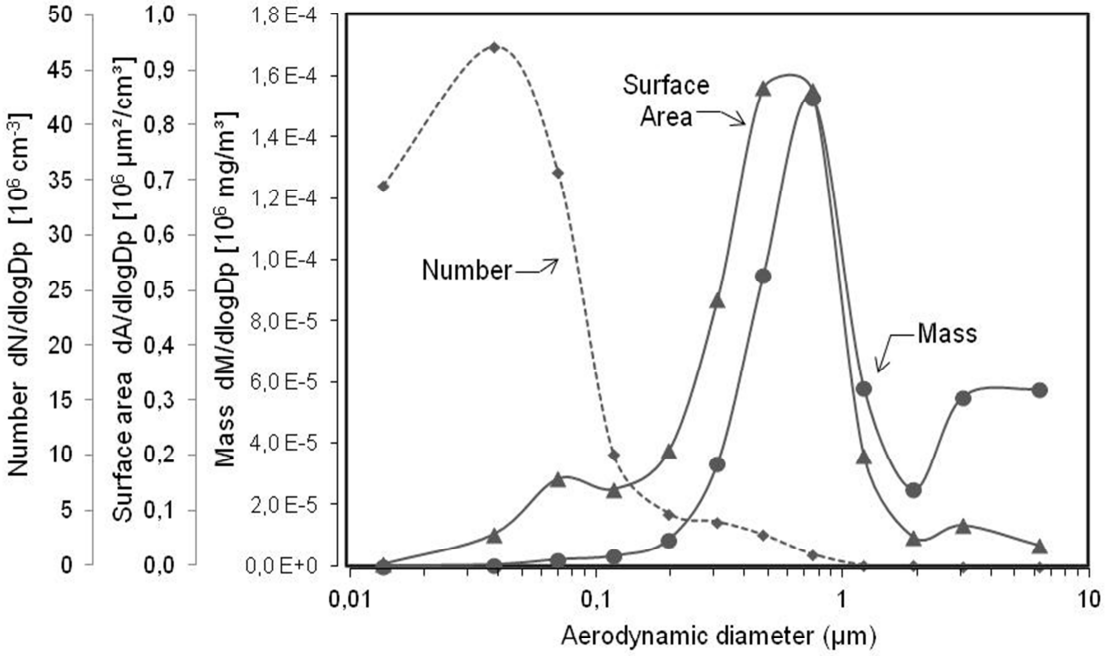

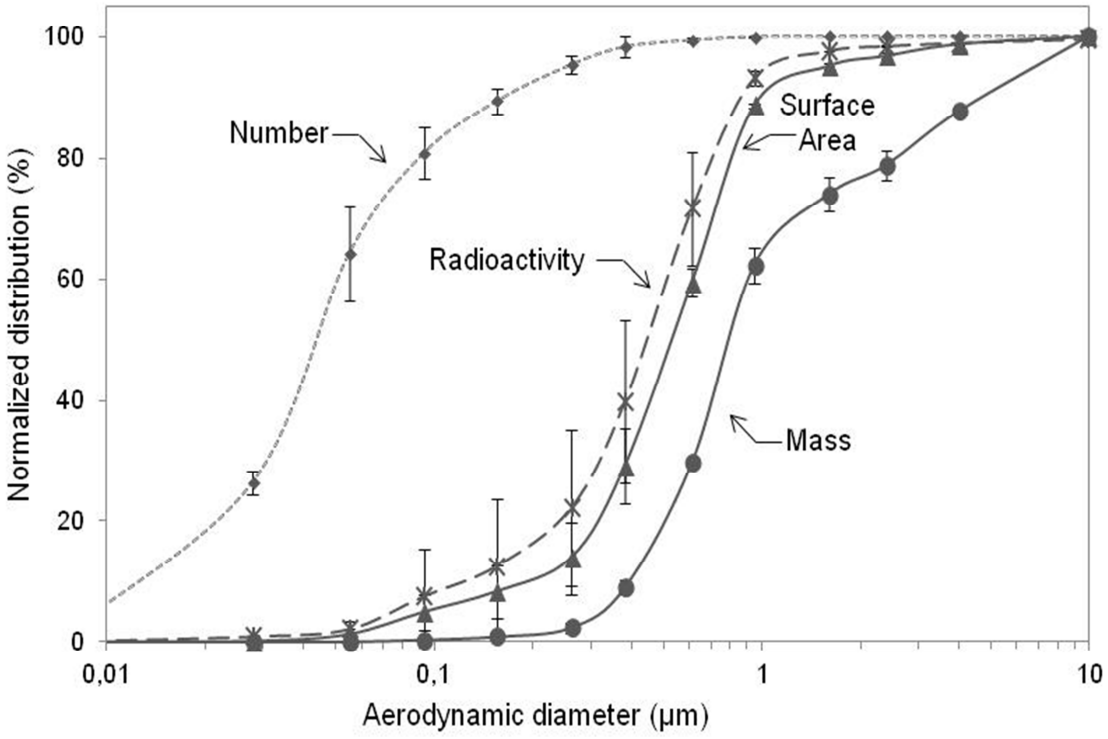

FIGURE 5. Radiolabelling efficiency expressed as activity per particle mass.

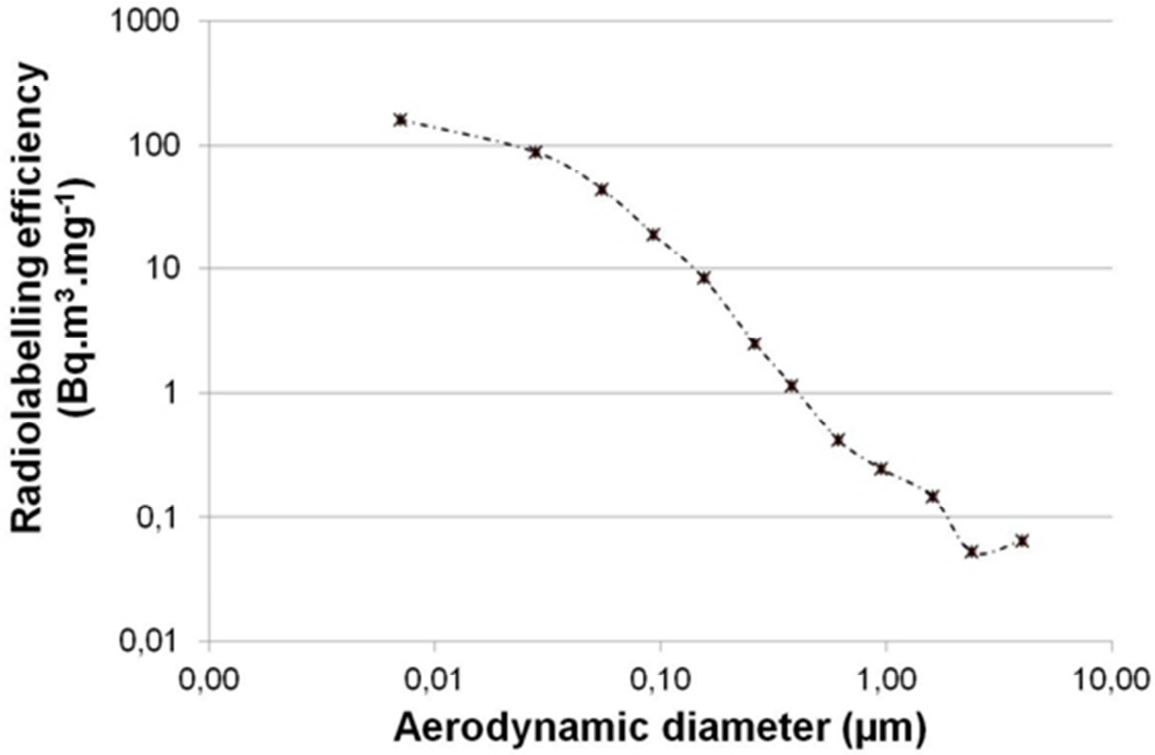

FIGURE 6. Operating parameters influencing Technegas aerodynamic particle size distribution. Clinical operating conditions are used as a reference (distribution in black bold line).

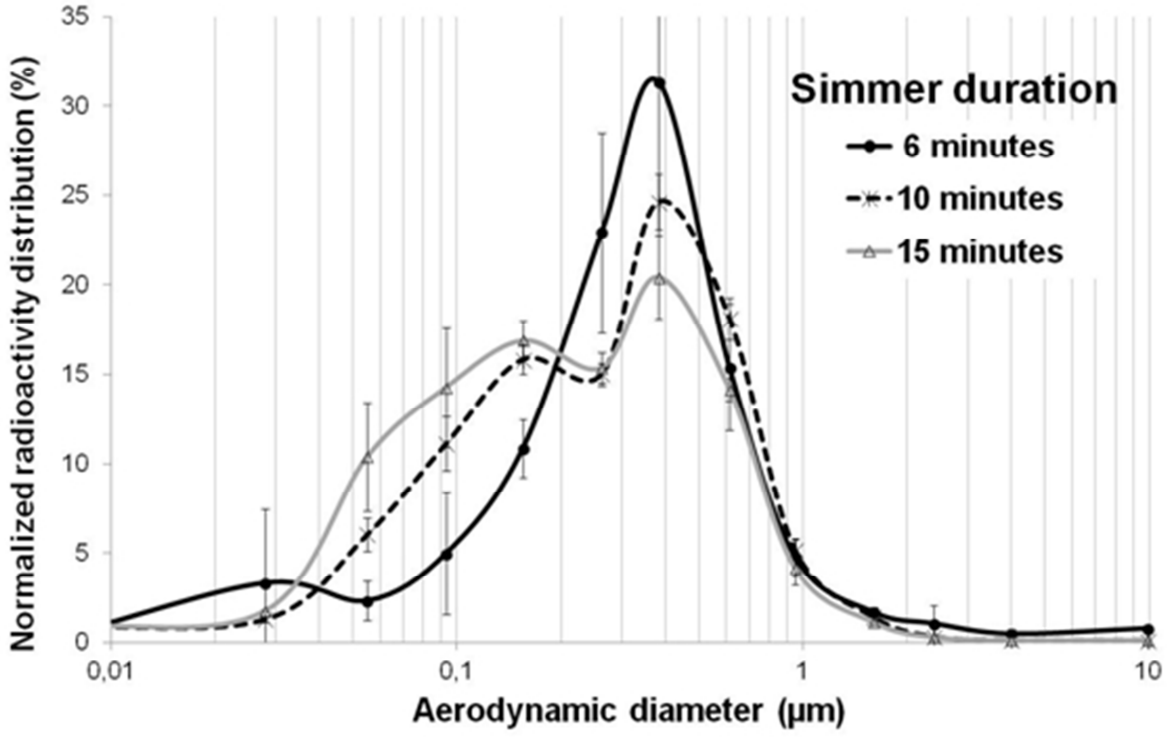

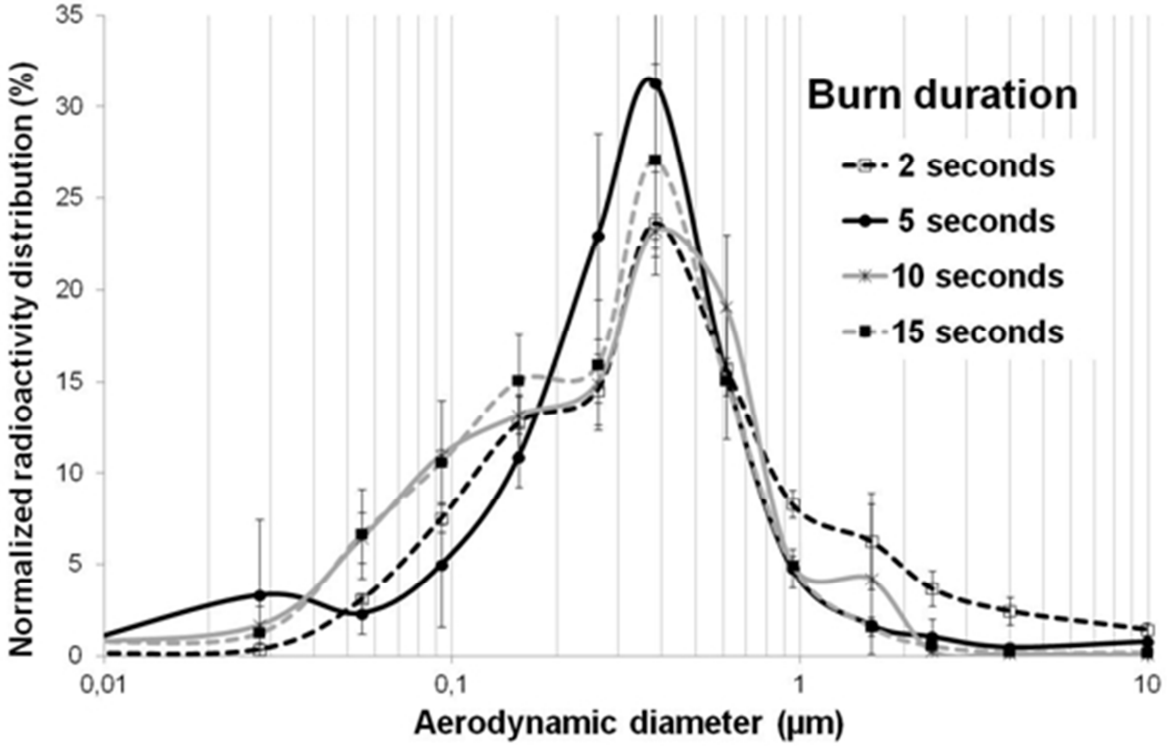

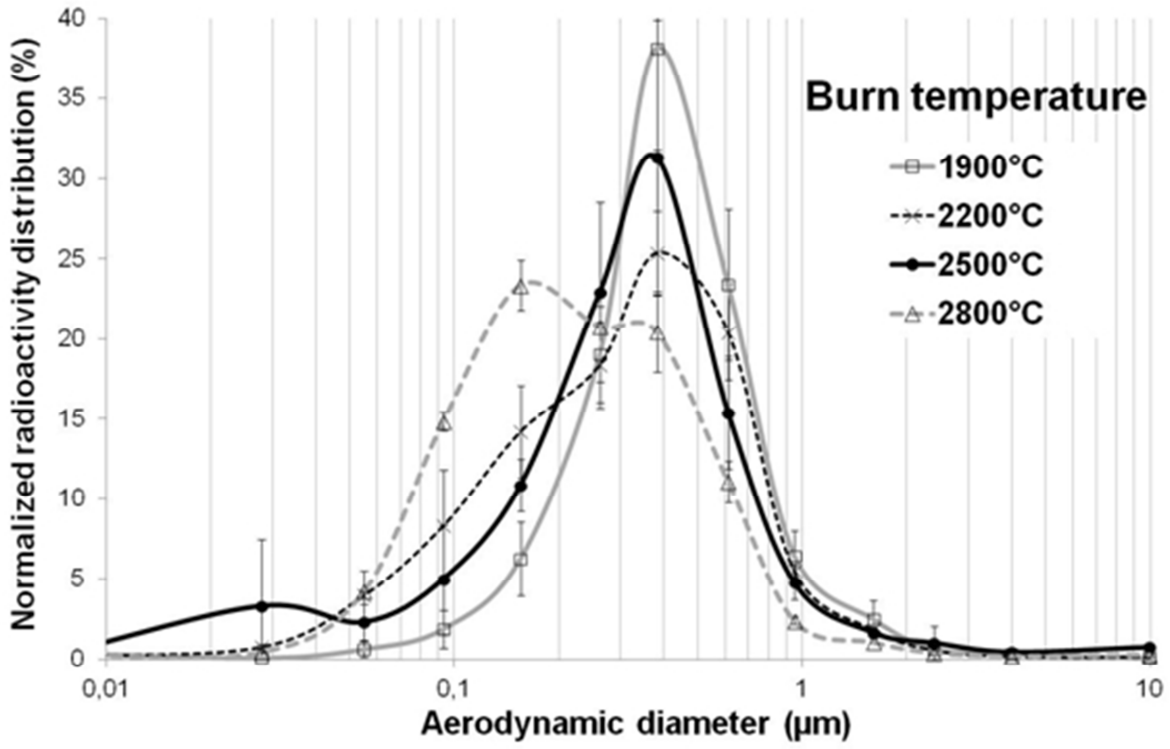
Burn temperature
1900°C
2200°C
2500°C
2800°C
Normalized radioactivity distribution (%)
Aerodynamic diameter (µm)
0
5
10
15
20
25
30
35
40
0,01
0,1
1
10

29

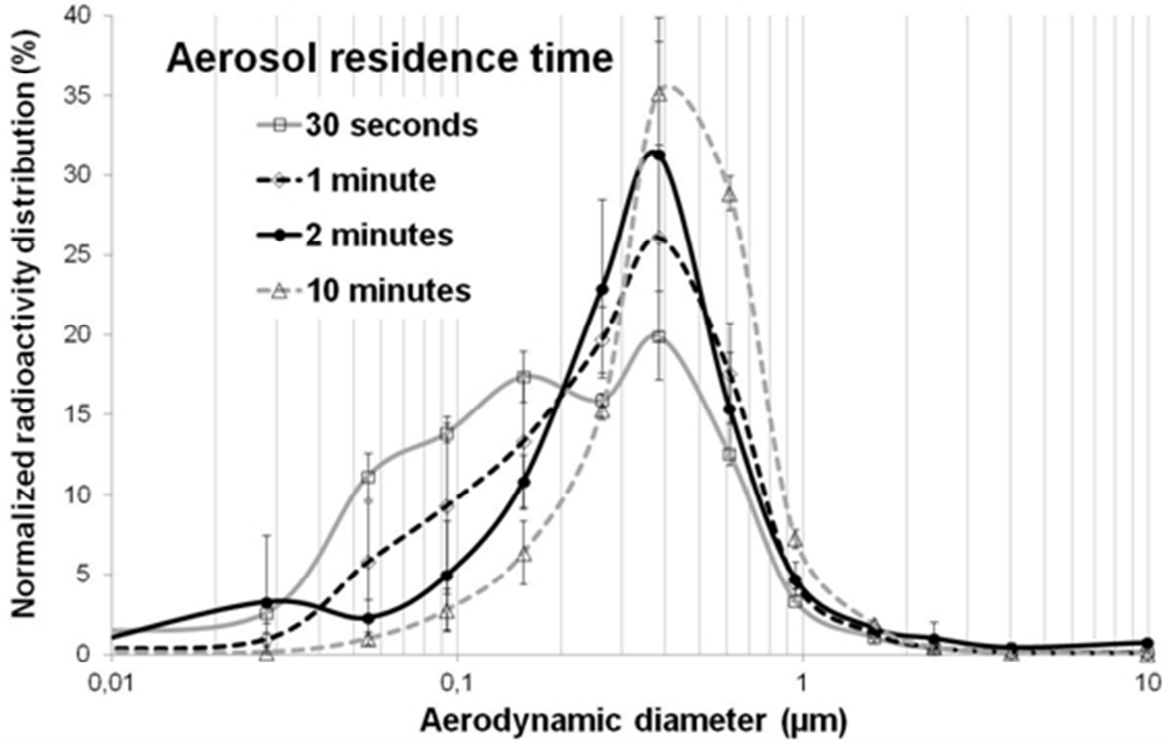
Aerosol residence time
30 seconds
1 minute
2 minutes
10 minutes
Normalized radioactivity distribution (%)
Aerodynamic diameter (µm)
0
5
10
15
20
25
30
35
40
0,01
0,1
1
10

30

31

32

FIGURE 7. SEM images of particles deposited on ELPI stage corresponding to mid-point aerodynamic diameter of 2.39 µm for residence times of (A) 30 seconds and (B) 10 minutes. Arrows indicate agglomerated particles.

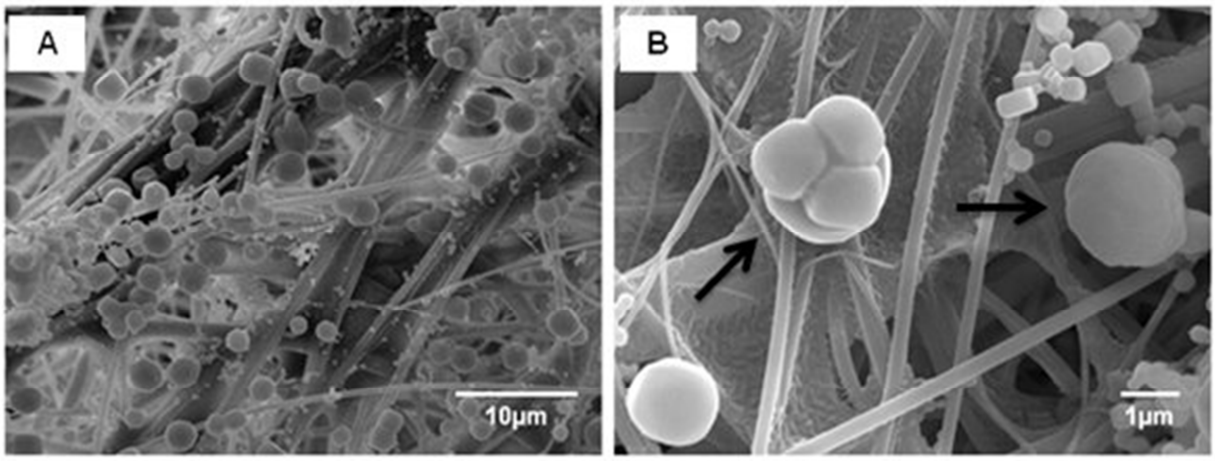

FIGURE 8. Total radioactivity of evaluated radio-aerosols: influence of operating parameters (* : Values are not significantly different, p<0.05).

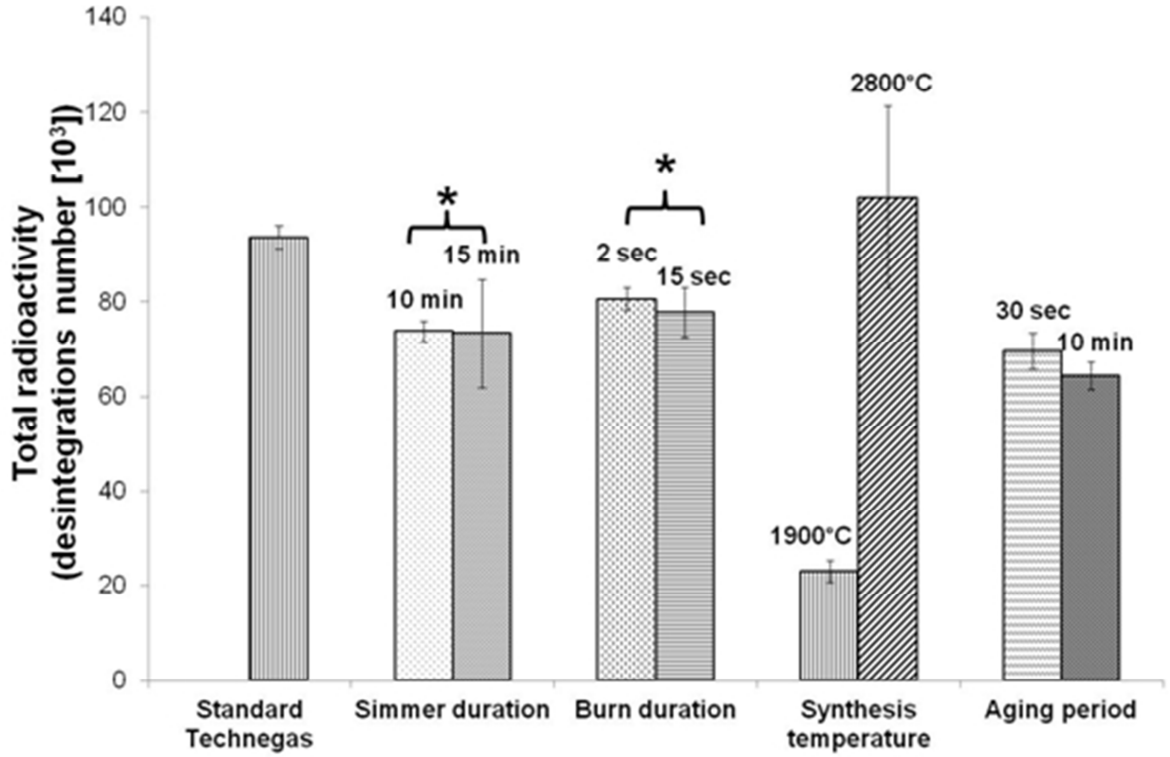

FIGURE 9. Technegas aerodynamic particle size distribution: comparison between standard clinical production, optimized production and optimized production using NaCl free-eluate.

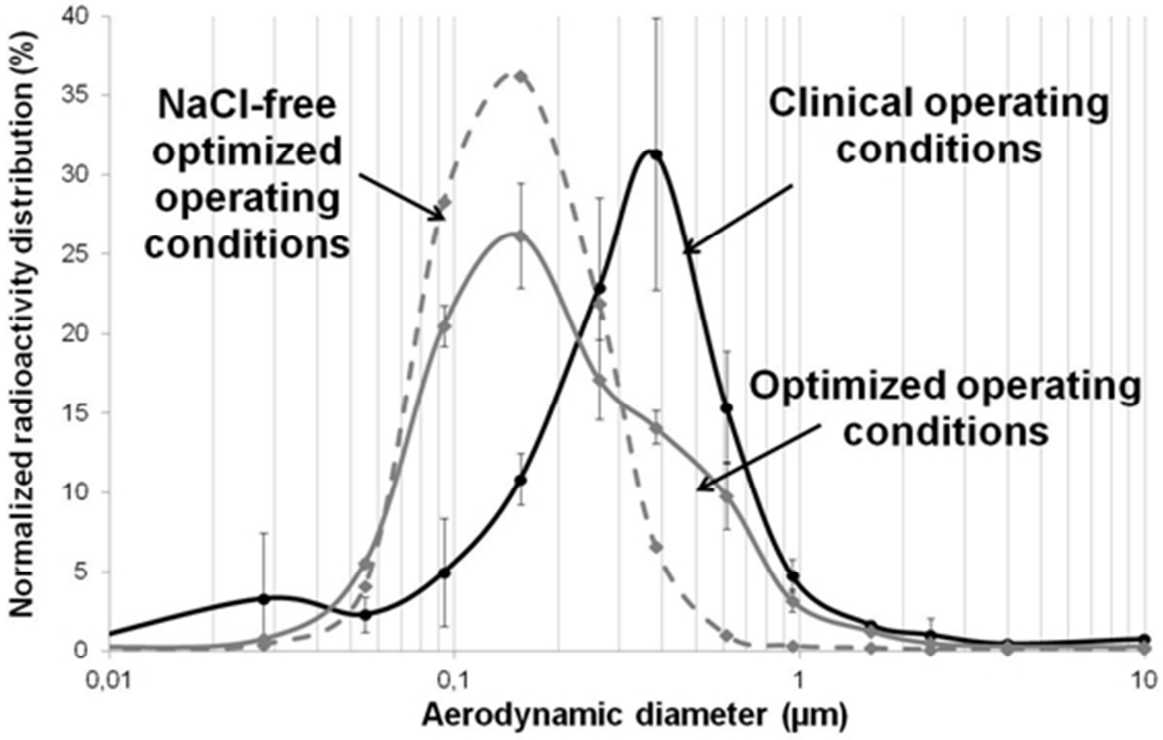

TABLE 1. Influence of ELPI collection substrates on aerosols particle size distributions: radioactivity median aerodynamic diameters (AMAD) and geometric standard deviation (GSD).

Generation Mode	ELPI Measurements	AMAD (nm)	GSD
standard clinical operating conditions	*without collection substrates*	450*	3.4
	with collection substrates	445*	3.0

* : values are not significantly different ($p<0.05$)

TABLE 2. Radioactivity median aerodynamic diameters (AMAD) and geometric standard deviation (GSD) under standard clinical operating conditions, or under modified and optimized operating conditions (modified generation parameters in bold).

	Generation parameters				Particle size distribution	
Analyzed parameters	Simmer duration (min)	Burn duration (s)	Synthesis temperature (°C)	Residence time (min)	AMAD (nm)	GSD
Standard	6	5	2500	2	450	2.7
Simmer duration	**10**	5	2500	2	380*	2.1
	15	5	2500	2	305	2.2
Burn duration	6	**2**	2500	2	500	3.2
	6	**10**	2500	2	385*	2.5
	6	**15**	2500	2	370	2.9
Synthesis temperature	6	5	**1900**	2	510	3.0
	6	5	**2200**	2	420	2.5
	6	5	**2800**	2	270	2.7
Residence time	6	5	2500	**0.5**	285	2.8
	6	5	2500	**1**	380*	2.5
	6	5	2500	**10**	540	2.6
Optimized	6	10	**1900°C followed by 2800°C**	2	250	2.5

* : values are not significantly different ($p<0.05$)